Gas Electron Multipliers in a Time Projection Chamber

by

Kasey Josephine Ensslin

Submitted to the Department of Physics
in partial fulfillment of the requirements for the degree of

Bachelor of Science in Physics

at the

MASSACHUSETTS INSTITUTE OF TECHNOLOGY

February 2003

Author .....
Department of Physics
January 21, 2003

Certified by .....
Ulrich J. Becker
Professor, Department of Physics
Thesis Supervisor

Accepted by .....
David Pritchard
Senior Thesis Coordinator, Department of Physics

Gas Electron Multipliers in a Time Projection Chamber

by

Kasey Josephine Ensslin

Submitted to the Department of Physics
on January 21, 2003, in partial fulfillment of the
requirements for the degree of
Bachelor of Science in Physics

Abstract

A nine liter Time Projection Chamber (TPC) containing both a Gas Electron Multiplier (GEM) and signal wires was used to reconstruct tracks from alpha particles and cosmic ray muons. The maximum energy from an ^{241}Am source is 5.5 MeV, but some of this energy is lost due to the finite thickness and coating of the source. Measurements of alpha ranges were taken in gas mixtures of Ar:C_2H_6 (50:50), Ar:CH_4 (90:10), and Ne:CH_4 (90:10). The measured ranges were 2.8 ± 0.5 cm, 3.2 ± 0.5 cm and 4.8 ± 0.5 cm respectively. These values correspond to 4.3 MeV alpha ranges from NIST's Physical Reference Data [1] indicating that 1.2 MeV is lost emerging from the source. Alpha track measurements demonstrate that a TPC with a GEM is a viable tracker. Alpha measurements also provided an estimate of the gain from the GEM as well as the wires. The gain from both the GEM and the wires was smallest in Ar:C_2H_6 (50:50), larger in Ar:CH_4 (90:10), and largest in Ne:CH_4 (90:10), suggesting that a neon mixture is well suited for use in future detectors. Cosmic ray muon tracks were measured in Ar:CH_4 (90:10) as an example of minimum ionizing particles. The GEM TPCs are new developments for tracking detectors in the planned TeV Linear Collider.

Thesis Supervisor: Ulrich J. Becker
Title: Professor, Department of Physics

Acknowledgments

I would like to thank Prof. Ulrich Becker for making this thesis possible. I would also like to thank Profs. Peter Fisher and Kate Scholberg for their help and support. I would like to recognize the support of the Microsystems Technology Laboratory for the use of their facilities. Thanks also goes to Josh Thompson for his previous work on this experiment and all the other students in Building 44, Gianpaolo Carosi, Bilge Demirköz, Reyco Henning, Ben Monreal, Jennifer Lue and James Pate.

Contents

List of Figures

List of Tables

Chapter 1

Introduction

1.1 TPC as a Particle Detector

A Time Projection Chamber (TPC) is a type of drift chamber used to reconstruct a three dimensional particle track. A TPC typically consists of a large volume of gas for ionization with one side covered by sense wires and a pad plane. A field cage creates a uniform electric field in the drift region and causes electrons to drift towards the wires and pads. A TPC works based on the time projection principle, which is illustrated in Fig. 1-1 [2]. In the vicinity of the wires, the high electric field creates secondary electron ionizations which form an avalanche. 10^2-10^6 secondary electrons are created in a process called gas amplification. The avalanche causes a current in the wires (y coordinate) and an induced charge on the pads (x coordinate). First a two dimensional track is found from the grid of pad data. Next, timing information is used to create a three dimensional track. Based on their large detection volume and simple 3D track reconstruction, TPCs are very useful particle detectors. This thesis uses a nine liter TPC built by U. Becker and V. Koutsenko as a prototype for a space experiment [6] and used by J. Thompson [2]. The TPC was modified by introducing a Gas Electron Multiplier (GEM) to increase gas amplification.

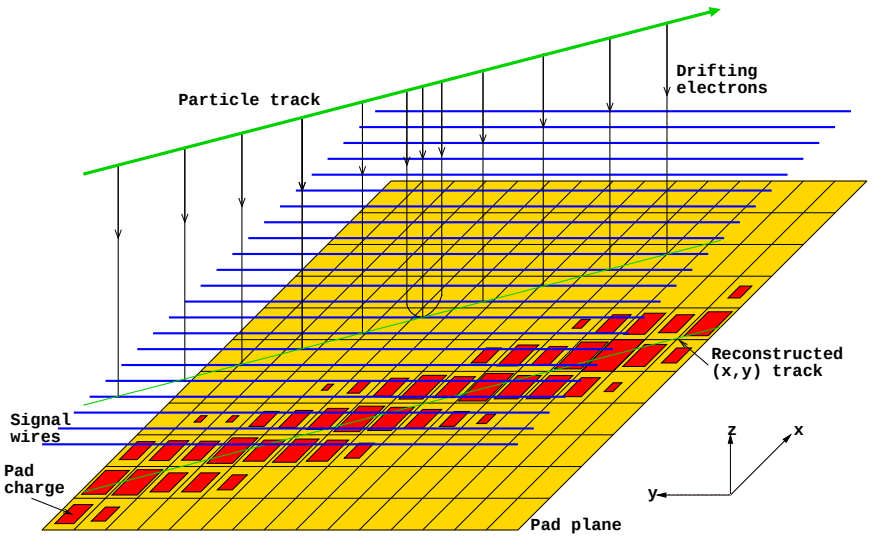

Figure 1-1: Creation of a three-dimensional particle track in a TPC [2].

1.2 Energy Loss in the Bethe-Bloch Formula and Particle Ranges

Since TPCs are often used to measure particle ranges, it is important to understand the expected range of different particles. The range of a particle is related to the rate of energy loss, dE/dx by the following integral,

$$R = \int_0^{T_0} \frac{1}{dE/dx} dE, \tag{1.1}$$

where T_0 is the energy of the particle [7].

The rate of energy loss of a particle can be calculated from the Bethe-Bloch equation,

$$-\frac{dE}{dx} = 2\pi N_A r_e^2 m_e c^2 \frac{Z}{A}\frac{z^2}{\beta^2}\left(\ln\frac{2m_e c^2\beta^2\gamma^2 W_{max}}{I^2} - 2\beta^2 - \delta\right). \tag{1.2}$$

Here $2\pi N_A r_e^2 m_e c^2 = 0.1535$ MeVcm^2/g and r_e is the classical electron radius (2.817 x 10^{-13} cm), m_e is the electron mass, N_A is Avogadro's number, I is the mean excitation potential, Z is the atomic number of the absorbing material, A is the atomic mass of the absorbing material, z is the charge of the incident particle in

Energy [MeV]	Ar:C_2H_6 (50:50)	Ar:CH_4 (90:10)	Ne:CH_4 (90:10)
		Ranges [cm]	
4.0	2.3	2.8	4.4
4.3	2.6	3.2	4.8
4.5	2.8	3.4	5.1
5.0	3.2	3.9	5.9
5.5	3.7	4.5	6.8

Table 1.1: Ranges of alpha particles in cm in three gases at energies of 4-5.5MeV [1].

units of e, β is the velocity of the incident particle in units of c, $\gamma = \frac{1}{\sqrt{1-\beta^2}}$, δ is the density correction and W_{max} is the maximum energy transfer in a single collision [7].

For non-relativistic particles, dE/dx decreases as $1/\beta^2$, but dE/dx in Eqn. 1.2 hits a minimum around $\gamma = 3$ and is relatively flat thereafter. Some cosmic ray muons have an energy near the minimum dE/dx, but most have an energy above it. Because many occur near the minimum, they are called minimum ionizing particles.

For less relativistic particles such as 5.5 MeV alphas, the Bethe-Bloch formula is not valid and it is necessary to use empirical data for the energy loss to calculate the range. The ranges of alpha particles have been measured and can be found online [1]. For a 5.5 MeV alpha particle, the range in argon is 7.508 x 10^{-3} gm/cm^2, in neon the range is 6.327 x 10^{-3} gm/cm^2 and in methane the range is 3.142 x 10^{-3} gm/cm^2. There was no data for the range in ethane, but the range in ethylene is 3.660 x 10^{-3} gm/cm^2. [1] The range of an alpha particle in the gas mixtures used in this thesis can be found by dividing by the gas density and multiplying by the percentages. The ranges for each gas at energies of 4-5.5 MeV are given in Table 1.1.

[1] There were two calculations of the range for each material. The one quoted here was calculated using the continuous-slowing-down-approximation (CSDA) which integrates the reciprocal of the total stopping power (collision plus nuclear) with respect to energy. The projected range was also listed. Projected ranges are calculated using the elastic scattering cross sections. The projected ranges for argon, neon, methane and ethylene are 7.358 x 10^{-3} gm/cm^2, 6.250 x 10^{-3} gm/cm^2, 3.134 x 10^{-3} gm/cm^2, and 3.648 x 10^{-3} gm/cm^2 respectively [1].

1.3 GEM: A New Device

Description

Gas Electron Multipliers (GEMs) are relatively new devices capable of gas amplification and can be used to replace signal wires. A GEM typically consists of a thin sheet of kapton [8] ($\sim$ 50 μm thick), copper clad on both sides ($\sim$ 2 μm thick), with a honeycomb pattern of conical holes etched throughout [9]. The holes in the copper must be larger than the holes in the kapton to prevent electrical sparking (copper hole $\sim$ 72 μm, kapton hole $\sim$ 41 μm). The holes in the kapton and copper were measured under a microscope as described in Appendix C. The honeycomb pattern and a schematic of a single GEM hole is shown in Fig. 1-2.

With a potential difference between the two copper sheet coatings, this geometry creates very strong electric fields inside the holes which in turn creates an avalanche of electrons. An order of magnitude estimate of the field strength is given by the GEM voltage divided by the thickness: $E_{center} \sim \frac{500V}{50\mu m} \sim 100\frac{kV}{cm}$. This provides the electrons with a typical mean free path of 4 μm (at 1 atm) and an energy of 40eV. This is sufficient to cause secondary ionization. More detailed calculations of the field strength were done by Peter Fisher using the program Maxwell 3D, as is discussed in Appendix D [4].

Why GEMs?

GEMs have advantages over traditional wire amplification. The main advantage is that there are no wires to break. Another advantage is that GEMs prevent positive ions from drifting into the detection region and causing field distortion by the accumulation of static charge. In wire based TPCs, a grounded mesh is typically present to suppress the migrating positive ions, but a GEM does this more efficiently.

GEMs are have the advantage that their electric field is more uniform that the field from a traditional wire detector. The electric field from a wire is $E \propto \frac{1}{r}$, whereas the electric field from a GEM is roughly uniform except for the perturbation from the holes.

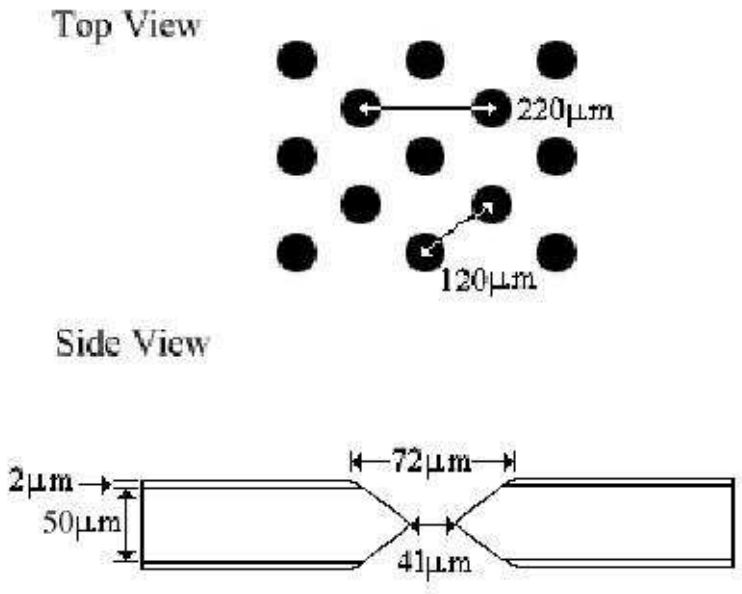

Figure 1-2: Hole pattern and schematic of a single hole.

Another advantage of GEMs is that they can be cascaded to achieve gains $\sim 10^3$ at stable operating conditions [9]. Some experiments use cascades of 2-4 GEMs in place of the wires inside a TPC [10].

1.4 Existing Experiments and Future Uses

Wire TPCs have recently been used in several major experiments. The PEP-4 detector at SLAC [11] was the first to use a TPC. The ALEPH and DELPHI experiments at CERN [12, 13] also used TPCs as trackers. The ALEPH experiment used a mixture of Ar:CH_4 (91:9) [14], which is close to the Ar:CH_4 (90:10) mixture used in this thesis. The DELPHI experiment used a mixture of Ar:CH_4 (80:20) [15]. Today, TPCs are used for studying heavy-ion collisions in such experiments as the STAR detector at the Relativistic Heavy Ion Collider (RHIC) at Brookhaven [16].

GEM TPCs are planned for NLC (US) and TESLA (DESY) and triple GEMs of

Sauli [9] are used in the COMPASS experiment at CERN. The GEM in this thesis has the exact same hole pattern and geometry as those used in COMPASS.

Chapter 2

Apparatus

2.1 TPC at MIT

A TPC consisting of a cage structure creating a drift field, followed by a mesh, wires and a pad plane existed at MIT as shown in Fig. 2-1. The TPC was built by V. Koutsenko and U. Becker for gas studies [6]. Joshua Thompson took measurements with this conventional TPC with alpha tracks from an ^{241}Am source and muon tracks from cosmic rays [2].

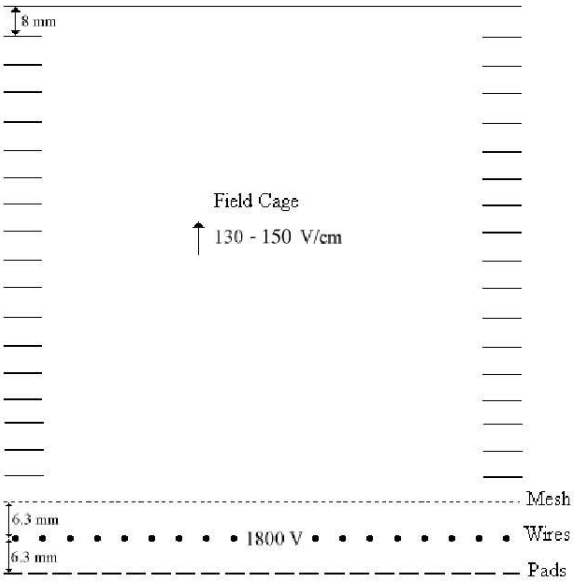

Figure 2-1: Schematic of Wire TPC [2].

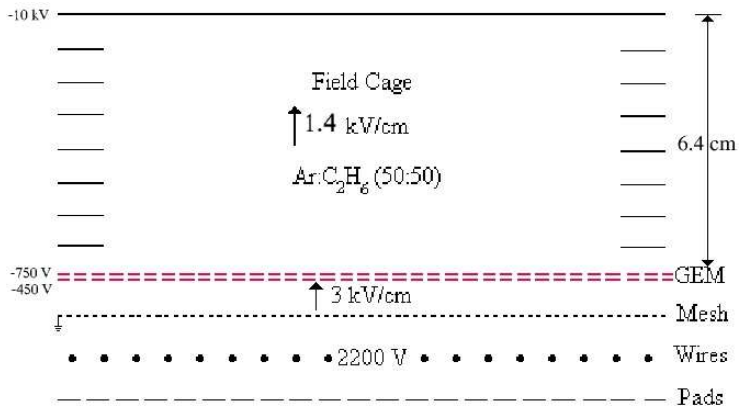

Figure 2-2: Schematic of the GEM TPC with wires and mesh.

This thesis deals with the innovation of introducing GEMs into the wire TPC. The GEMs used in this thesis were obtained from CERN [9, 17]. They are 10cm x 10cm with 72 μm holes in the copper and 41 μm holes in the kapton. These hole sizes were measured as described in Appendix C. Before the GEMs could be used, they were stretched and attached to frames, as described in Appendix A and they were electrically tested as described in Appendix B. It is necessary to keep the GEMs clean and free of dust, so they were inserted into the TPC using the clean room in the Microsystems Technology Laboratory at MIT.

A single GEM was added to the TPC leaving the mesh and signal wires in place. This was the first step towards creating wireless TPCs. The GEM was added below the drift field and above the mesh as show in Figs. 2-2 and 2-3. Thus a transfer field was established between the GEM and the grounded mesh. For this thesis, the transfer field was set at $E_T = 3kV/cm$. This field was chosen because it has to be high enough to transport electrons, but a larger field would have been prone to sparking due to the small distance (1.6 mm) between the GEM and the mesh.

The drift cage used in the wire TPC was 18 cm high and was connected to a 6kV supply. Alpha tracks were not visible using this large field cage with a drift field $\sim$150 V/cm. Most other GEM TPCs had drift fields of the same order as the transfer field, both of which were 1-3 kV/cm [18, 19]. Therefore, the size of the drift region was decreased to 6.4 cm and the cathode voltage supply was increased to 10 kV. With

the new configuration, the drift field can go up to $E_D = 1.4kV/cm$.

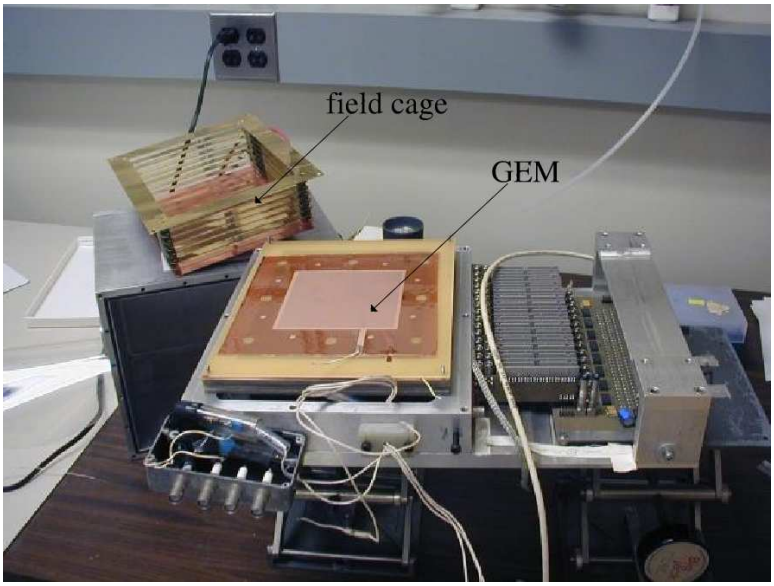

Figure 2-3: TPC with field cage removed to show GEM.

2.2 Discussion of Drift Gases

A drift gas for use in a TPC must have a large velocity at low electric fields so that the required voltages are reasonable. For the proposed detector in the Linear Collider (LC), a gas with a high drift velocity is also desired so that the electrons from the previous event are cleared quickly [20]. For example, an equal mixture of argon and ethane has a high drift velocity at the drift field of ~0.4 kV/cm as can be seen in Fig. 2-4 [3].

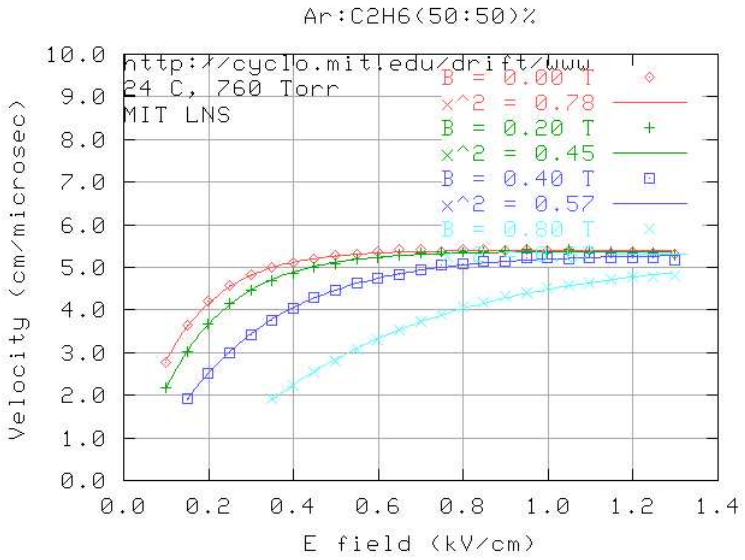

Figure 2-4: Measurement of drift velocity of Ar:C_2H_6 (50:50) from [3]. Only the B = 0 measurement is relevant here.

For the next LC, the tracker mixture should have low multiple scattering ($\propto Z^2$), which can be provided by a neon mixture. A helium mixture would be even better, except it does not have enough ionization. In addition, neon has distinctly advantageous amplification features [21, 22]. Therefore, some of the measurements are planned with a mixture of Ne:CH_4 (90:10). Measurements of the drift velocity for this gas can be seen in Fig. 2-5 [3]. Operation at 0.22 kV/cm is feasible.

For comparison with the neon mixture, some measurements were also taken with Ar:CH_4 (90:10), whose drift velocity can be seen in Fig. 2-6 [3] to have a maximum velocity at the stable operating point of 0.13 kV/cm.

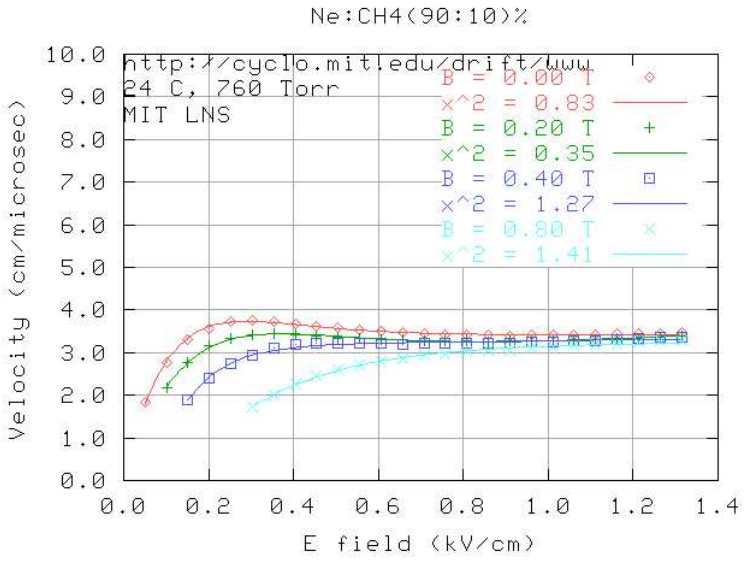

Figure 2-5: Measurement of drift velocity of Ne:CH_4 (90:10) from [3]. Only the B = 0 measurement is relevant here.

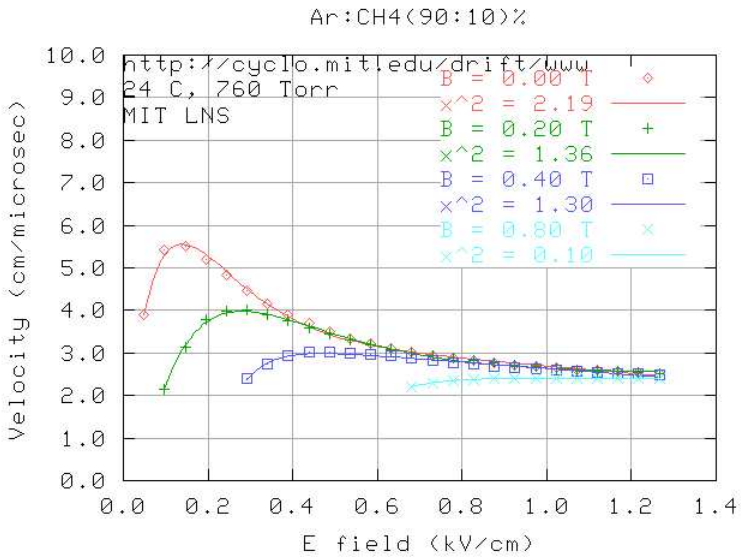

Figure 2-6: Measurement of drift velocity of Ar:CH_4 (90:10) from [3]. Only the B = 0 measurment is relevant here.

Chapter 3

Measurements and Analysis

3.1 Alpha Setup

Alpha particles emerge from an ^{241}Am source inside the TPC. The source, taken from a smoke detector, has finite thickness and coating so the energy is

$$5.5MeV - \int_{source} \frac{dE}{dx} dx. \tag{3.1}$$

The source is mounted on a metal bar attached in line with the field cage to form an equipotential and minimize the distortion to the drift field as shown in Fig. 3-1. The source is placed over the GEM so that the tracks, which are several centimeters long, are projected onto the pad plane. A diagram of the pad plane, complete with readout area, wire positions and alpha source, is shown in Fig. 3-2.

Since the alpha particles are stopped inside the TPC, no outside counter can be used as a trigger, therefore, it is necessary to trigger directly on the alpha wire signals. To measure alpha tracks, first it was determined that the tracks encountered wires 12-14, as shown in Fig. 3-3. Being closest to the source, wire 12 was chosen for the trigger.

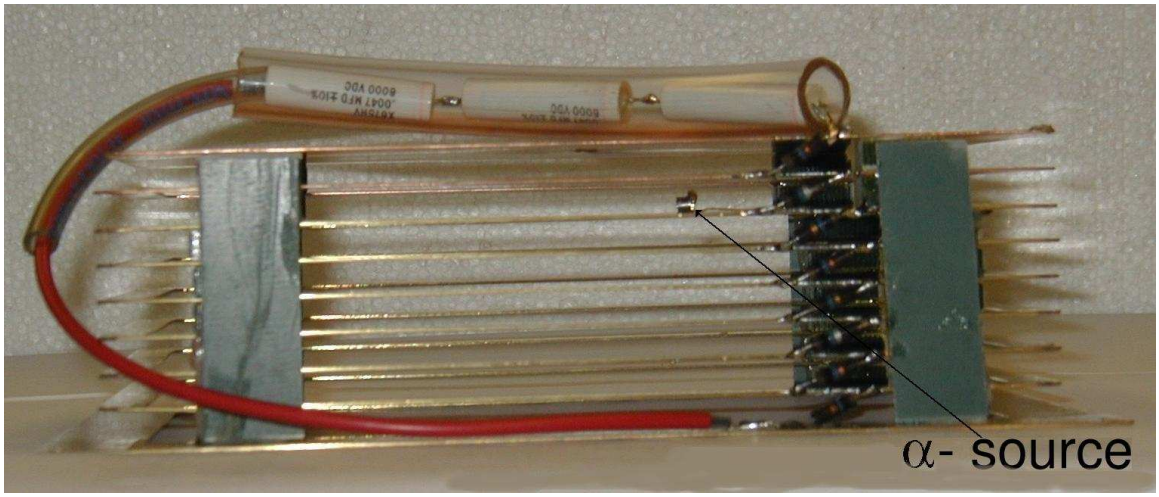

Figure 3-1: Alpha source mounted in field cage of TPC.

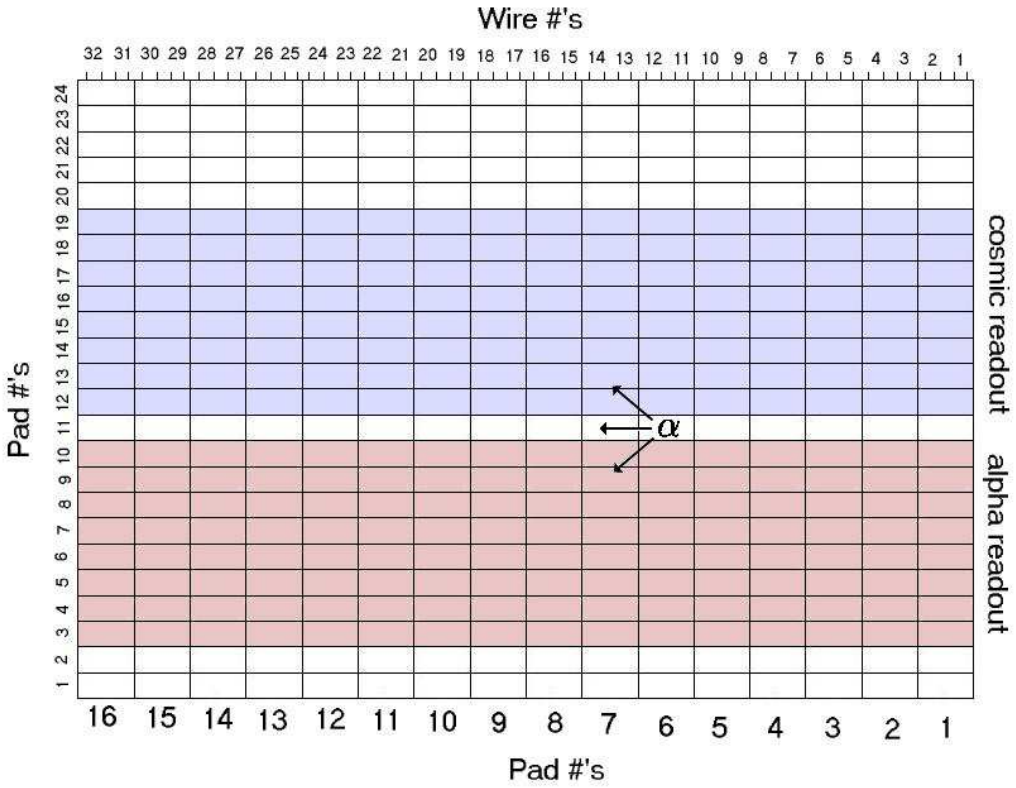

Figure 3-2: Pad plane with readout area, wire positions and alpha source shown.

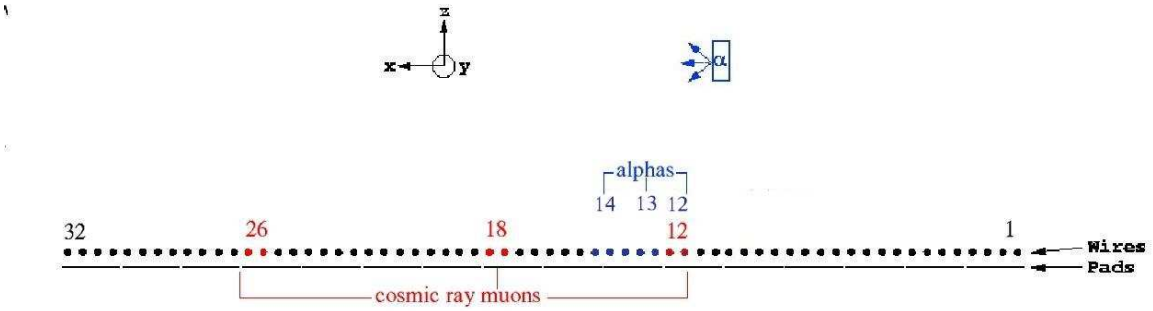

Figure 3-3: A diagram of the wires and pads, including those used for the alpha trigger. The numbers correspond to a pair of 30 μm wires, spaced 3 mm apart.

3.2 Determining Coordinates of Tracks

Wire signals for a sample α event are shown in Fig. 3-4 and the induced pad signals for the same event are shown in Fig. 3-5. The range of the alpha particles was determined from a combination of the pad data and the timing data from the oscilloscope. First the x and y coordinates were determined from the pad data. The y coordinate corresponds to the direction along the wires and the x coordinate is the pad dimension perpendicular to the wires. The pads are 12 mm long in the x direction and 6 mm long in the y direction. The x coordinate was determined by the number of pads encountered in the x-direction and the y coordinate was determined by a best fit line to the track. The best fit line was determined by calculating the centers of charge for each pad column. The x and y coordinates are shown in the sample pad data of Fig. 3-5.

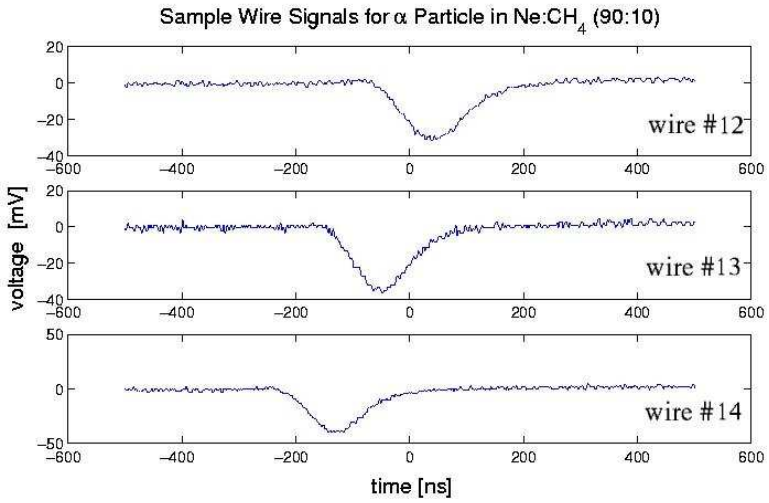

Figure 3-4: Sample of wire signals from an α event in Ne:CH_4 (90:10).

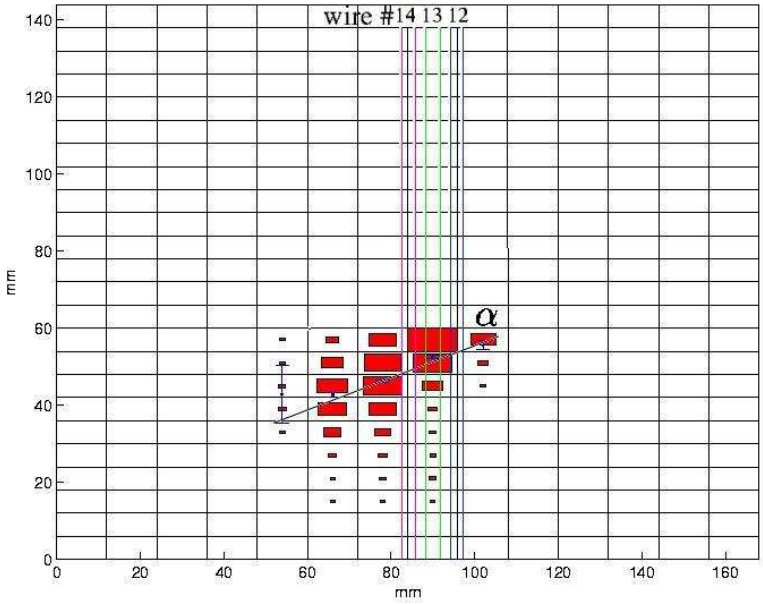

Figure 3-5: Sample of pad signals from an α event in Ne:CH_4 (90:10). The fully shaded pad has a charge of 107 pC and the charge on the other pads scales like the area.

The timing of the wire data, along with knowledge of the drift velocity ($v = 5cm/\mu s, 2.5cm/\mu s$, and $3.4cm/\mu s$, for Ar:C_2H_6 (50:50), Ar:CH_4 (90:10), and Ne:CH_4 (90:10) respectively), was used to find the z dimension, because

$$z = vt \tag{3.2}$$

where v is the drift velocity and t is the time between wire signals. The alpha particle show in Figs. 3-4 and 3-5 was traveling down because the signal on wire 10 is earliest and the signal on wire 8 is latest. If the signals had arrived in the opposite order, the alpha particle would have been traveling up.

The range was then calculated as

$$R = \sqrt{x^2 + y^2 + z^2}. \tag{3.3}$$

This calculation was made for 25 randomly chosen events in each gas; the ranges are listed in Table 3.1.

$Ar:C_2H_6$ (50:50)	$Ar:CH_4$ (90:10)	$Ne:CH_4$ (90:10)
1.7 ± 0.4	3.4 ± 1.8	3.0 ± 1.2
3.1 ± 1.3	3.8 ± 1.4	3.5 ± 1.1
1.5 ± 0.5	3.3 ± 1.4	3.7 ± 1.3
2.9 ± 0.9	3.7 ± 0.9	4.0 ± 1.4
2.2 ± 0.8	3.5 ± 1.4	4.1 ± 1.1
2.7 ± 0.8	3.2 ± 1.3	4.3 ± 1.5
4.0 ± 1.2	3.4 ± 1.0	4.3 ± 1.8
3.1 ± 1.0	2.7 ± 1.0	4.4 ± 1.1
2.5 ± 0.8	3.6 ± 0.9	4.5 ± 1.1
2.6 ± 0.8	2.7 ± 0.8	4.5 ± 0.8
3.2 ± 1.3	2.8 ± 0.9	4.6 ± 0.8
2.9 ± 0.9	3.4 ± 1.1	4.7 ± 0.8
2.5 ± 0.8	2.8 ± 0.5	4.7 ± 1.1
3.2 ± 1.3	3.2 ± 0.5	4.9 ± 0.7
2.9 ± 0.9	3.4 ± 1.1	5.0 ± 0.8
2.5 ± 0.8	4.0 ± 1.3	5.0 ± 0.9
3.5 ± 1.4	3.3 ± 1.4	5.1 ± 1.2
2.4 ± 0.8	3.8 ± 0.8	5.2 ± 0.7
2.8 ± 0.9	4.1 ± 1.3	5.2 ± 0.9
2.5 ± 0.8	4.6 ± 0.9	5.3 ± 0.8
2.2 ± 0.7	2.9 ± 0.6	6.1 ± 1.8
4.2 ± 1.7	4.3 ± 1.3	6.6 ± 1.5
2.4 ± 0.8	4.1 ± 1.4	8.4 ± 2.4
3.2 ± 1.0	3.5 ± 0.9	9.9 ± 1.9
2.6 ± 0.8	2.4 ± 0.8	10.0 ± 2.8

Table 3.1: Ranges and errors in cm for 25 events in each gas mixture.

3.3 Evaluation of Ranges

The data given in Table 3.1 was plotted in the histograms shown in Figs. 3-6, 3-7 and 3-8. A Gaussian was fitted to the data to determine the average range and errors. The range in Ar:C_2H_6 (50:50) was determined to be 2.8 $\pm$ 0.5 cm, the range in Ar:CH_4 (90:10) was determined to be 3.2 $\pm$ 0.5 cm, and the range in Ne:CH_4 (90:10) was determined to be 4.8 $\pm$ 0.5 cm. As was expected, these ranges are less than the ranges for 5.5 MeV alpha particles. This effect was also observed by Josh Thompson [2] and it was attributed to energy loss due to the thickness and coating of the source, as shown by Eqn. 3.1. Although we do not know the precise thickness of the source, we can show that even though the difference in the ranges is substantial, the mean energy is the same. The ranges determined here actually correspond to a mean energy of 4.3 MeV [1] as shown in Table 1.1. The ranges agree well within errors, so we conclude that a TPC with a GEM is a viable tracking device.

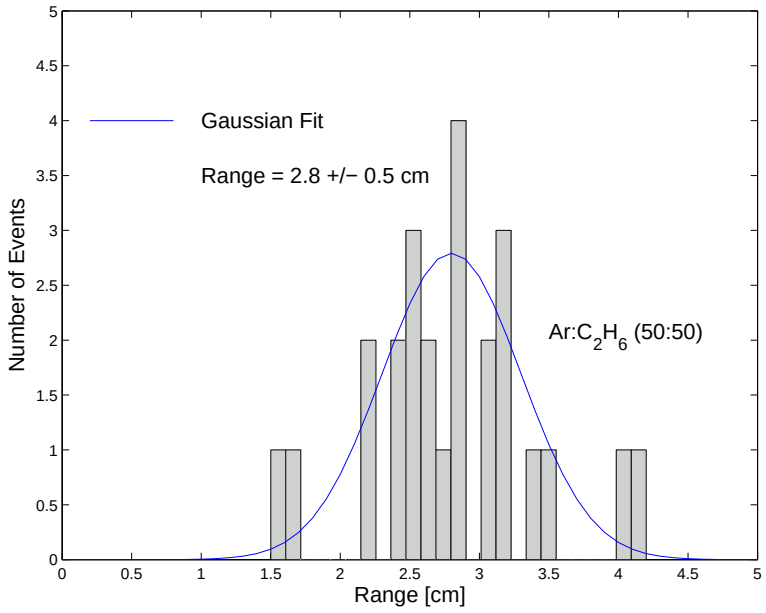

Figure 3-6: Histogram of alpha particle ranges in Ar:C_2H_6 (50:50).

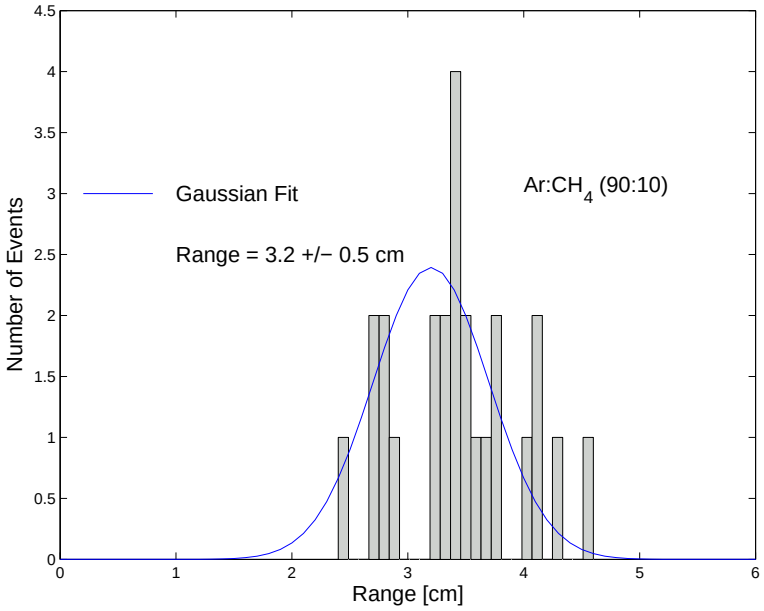

Figure 3-7: Histogram of alpha particle ranges in Ar:CH_4 (90:10).

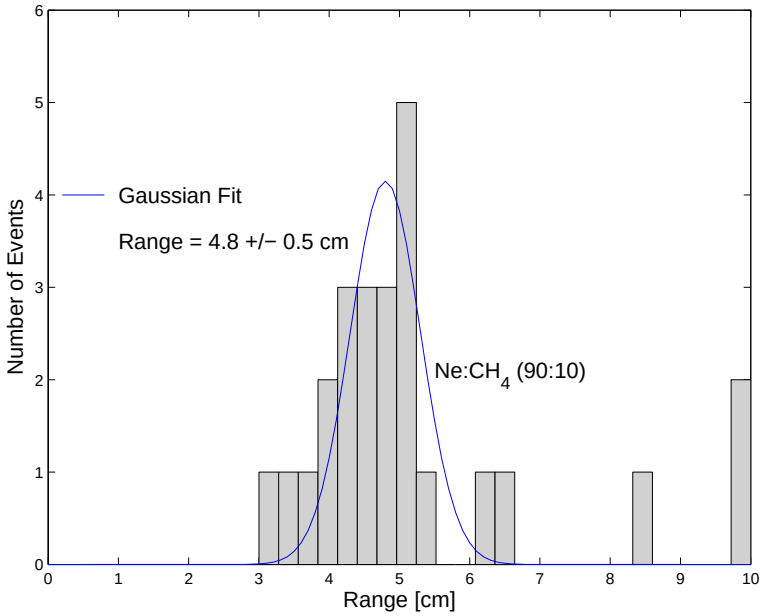

Figure 3-8: Histogram of alpha particle ranges in Ne:CH_4 (90:10).

3.4 Estimate of Gain

3.4.1 Gain

A naive estimate of the gain in the GEM can be found assuming that the mean free path for ionization is $\lambda = 7\mu m$. Since the GEM is $50\mu m$ thick, there will be approximately 7 ionizations on the path through the GEM. This yields a gain of $G \sim 2^7 = 128$. This is an over estimate of the gain because the electric field inside the holes is actually weaker than assumed here.

A better method for finding the gain is to use the First Townsend coefficient, α. This gives the number of electrons in the avalanche as:

$$dn = n\alpha dx, \tag{3.4}$$

where n is the number of electrons in the avalanche and x is the path length [7].

Therefore the gain can be written as:

$$G = \frac{n}{n_0} = e^{\int_{path} \alpha(E)dx}. \tag{3.5}$$

where n_0 is the number of primary electrons [7].

The gain of the GEM can be found by integrating Eqn. 3.4 and assuming a form of the Townsend coefficient as discussed in Appendix D.

Eqn. 3.5 can also be used to find the gain from a wire. This can be done by integrating directly, but is more often done using the Diethorn approximation that

$$\alpha(E) \approx \beta E \tag{3.6}$$

where β is a constant [23]. This approximation allows Eqn. 3.5 to be integrated to obtain Diethorn's Formula:

$$lnG = \frac{ln2}{ln\frac{b}{a}} \frac{V}{\Delta V} ln \frac{V}{ln\frac{b}{a} a E_{min}(\rho_0) \frac{\rho}{\rho_0}} \tag{3.7}$$

where b is the effective tube radius, a is the wire radius, V is the voltage, ΔV is the effective ionization potential, ρ is the gas density and E_{min} is the minimum electric field to cause ionizations [5].

Transfer Functions and Gain

The transfer function, $T(E)$, of a GEM describes what fraction of the electrons from the track are transfered through the GEM holes to the wires. Some electrons never make it to the readout because they crash into the upper GEM or are curled back to crash into the lower GEM. The observed gain from a GEM is actually a result of both the GEM amplification and the transfer function. Fig. 3-9 shows the electron paths through the GEM.

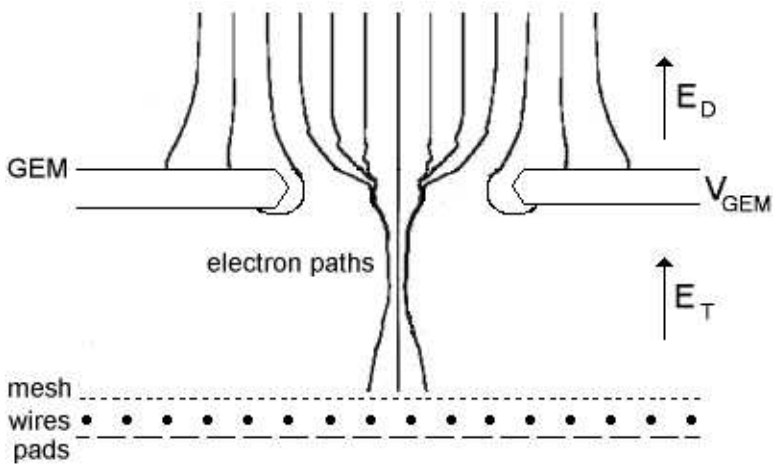

Figure 3-9: Schematic of electron paths through a GEM; does not include diffusion. Some electrons make it to the wires, but others are cut off at the top plate and others curl around and hit the bottom plate.

The amount of electrons which enter above the GEM is dependent only on the the drift field E_D. The fraction of these which go through the holes is described by $T_D(E_D)$. Let G_0 be the GEM amplification as described above and $T_T(E_T)$ be the transfer of electrons towards the readout plane. That is, the electrons which do not curve into the GEM. Taking these effects into account, the measured gain from a GEM should be

$$G_{eff} = T_D(E_D)G_0T_T(E_T). \tag{3.8}$$

A simulation of G_{eff} using electric fields calculated by the Maxwell 3D program along with assumptions about the Townsend coefficient was done by Peter Fisher at MIT [4]. This simulations are discussed in Appendix D.

Because there are wires in the TPC discussed here, the gain that I measure includes the gain from the wires, G_{wires}. The measured gain is therefore given by,

$$G(V_{wire}, V_{GEM}, E_T, E_D) = G_{wire}(V_{wire})G_{eff} = G_{wire}(V_{wire})T_D(E_D)G_0(V_{GEM})T_T(E_T). \tag{3.9}$$

3.4.2 Measurements of Gain

Alpha particle signals were measured in Ar:C_2H_6 (50:50), Ar:CH_4 (90:10), and Ne:CH_4 (90:10). For each gas, a measurement of pulse height versus wire voltage and of pulse height versus GEM voltage was taken. For these measurements the drift voltage was set to -10 kV, providing a drift field of $E_D = 1.4kV/cm$, and the lower surface of the GEM was set at -450 V, providing a transfer field of $E_T = 3kV/cm$. The voltage on upper surface of the GEM was varied to change the GEM voltage and the wire voltage was also varied to determine the relative values of G_{wire}. The factorization of Eqn. 3.9 is used to determine relative values of $G_0(V_{GEM})$ by variation of V_{GEM}, keeping all others the same and of $G_{wire}(V_{wire})$ by changing V_{wire} only.

Ar:C_2H_6 (50:50)

Fig. 3-10 shows two measurements of pulse height versus wire voltage for two different GEM voltage of 200 V and 300 V. Since E_T does not change and E_D only changes negligibly, the two measurements should only differ by the GEM amplification, which is 3.0 $\pm$ 0.3 in this case. Fig 3-11 shows measurements of GEM voltage versus pulse height for two different wire voltages. This graph gives a value of $\frac{\Delta G}{G\Delta V} = 0.008 \pm 0.0005\ \frac{1}{V}$, which is a measure of the change in gain for a given change in voltage.

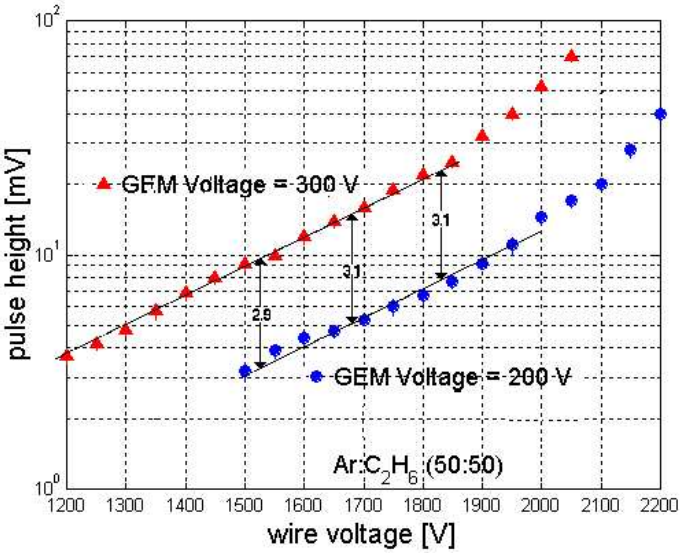

Figure 3-10: Pulse height versus wire voltage at constant GEM voltage in Ar:C_2H_6 (50:50).

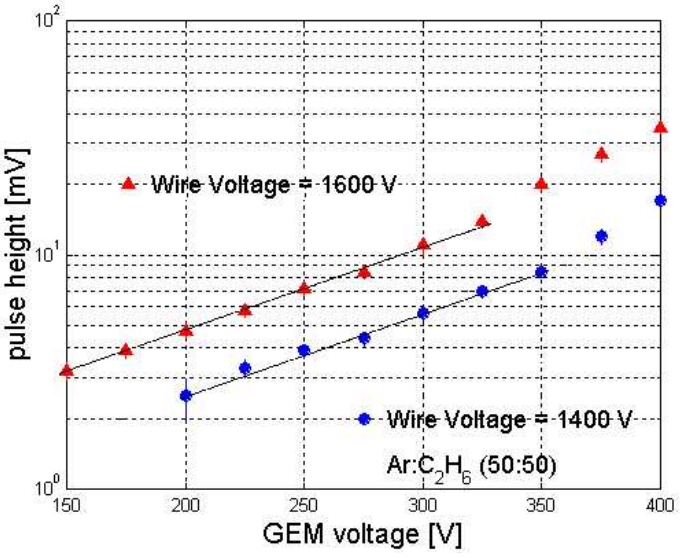

Figure 3-11: Pulse height and pad charge versus GEM voltage at constant wire voltages in Ar:C_2H_6 (50:50).

Ar:CH_4 (90:10)

Fig. 3-12 show measurements of pulse height versus wire voltage for GEM voltages of 200 V and 300 V. As discussed above, E_D and E_T are roughly constant, and therefore this graph gives a measurement of GEM amplification, which is 3.8 ± 0.3 in this case. Fig. 3-13 gives two measurements of pulse height versus GEM voltage. This graph gives a value of $\frac{\Delta G}{G \Delta V} = 0.016 \pm 0.004 \ \frac{1}{V}$.

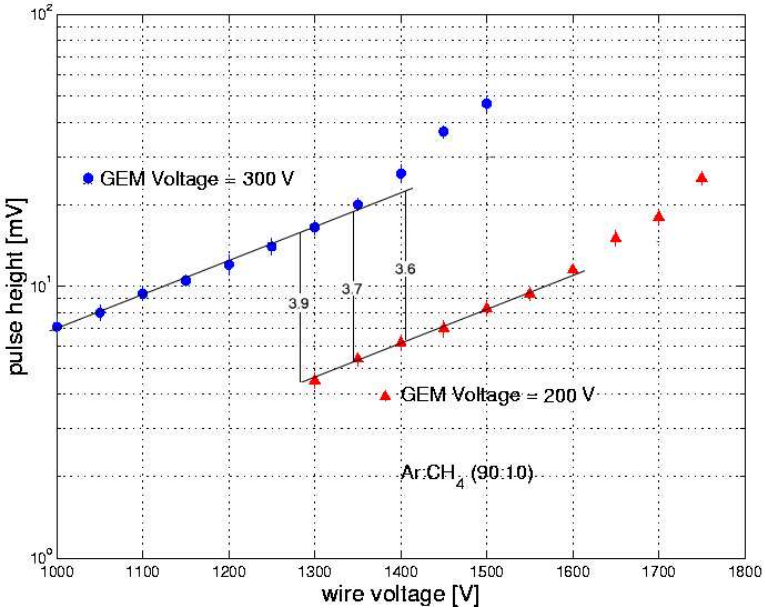

Figure 3-12: Pulse height versus wire voltage at constant GEM voltage in Ar:CH_4 (90:10).

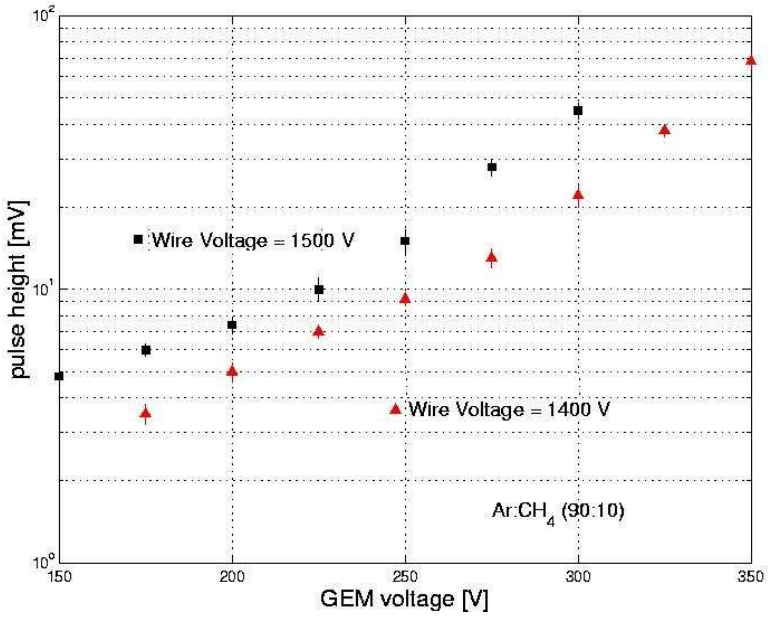

Figure 3-13: Pulse height and pad charge versus GEM voltage at constant wire voltages in Ar:CH_4 (90:10).

Ne:CH_4 (90:10)

Fig. 3-14 gives measurements of pulse height versus wire voltage at constant GEM voltages of 200 V and 250 V. There is an increase of 2.0 $\pm$ 0.3 between the two measurements which can be attributed to GEM amplification. Fig. 3-15 shows measurements of pulse height versus GEM voltage at three different wire voltages. They are not parallel at low GEM voltages, but this can be attributed to insufficient GEM amplification, which will occur when the electron cannot pick up enough energy in a mean free path to cause ionization. This graph gives a value of $\frac{\Delta G}{G \Delta V} = 0.025 \pm 0.005 \ \frac{1}{V}$ which is higher than the other gases.

Given exact knowledge of the electric field along the path, this data could be used to extract the Townsend coefficient $\alpha(E)$ for low electric fields in neon.

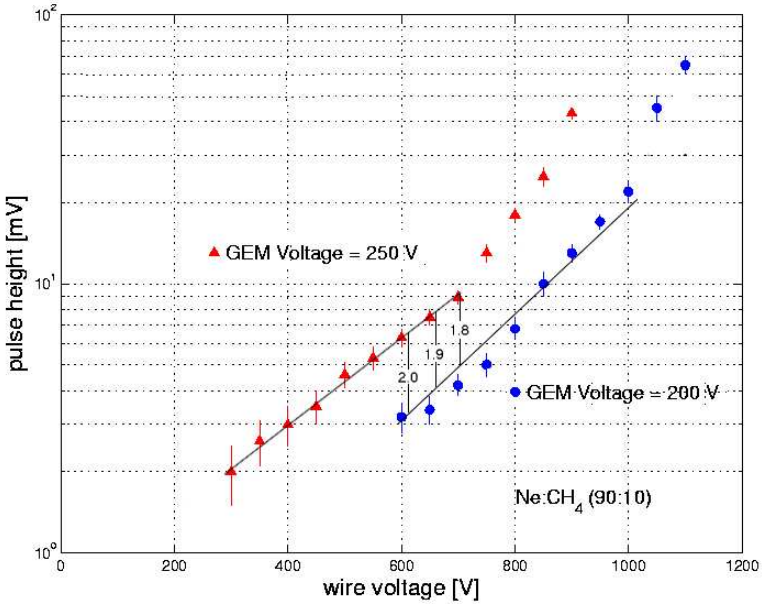

Figure 3-14: Pulse height versus wire voltage at constant GEM voltage in Ne:CH_4 (90:10).

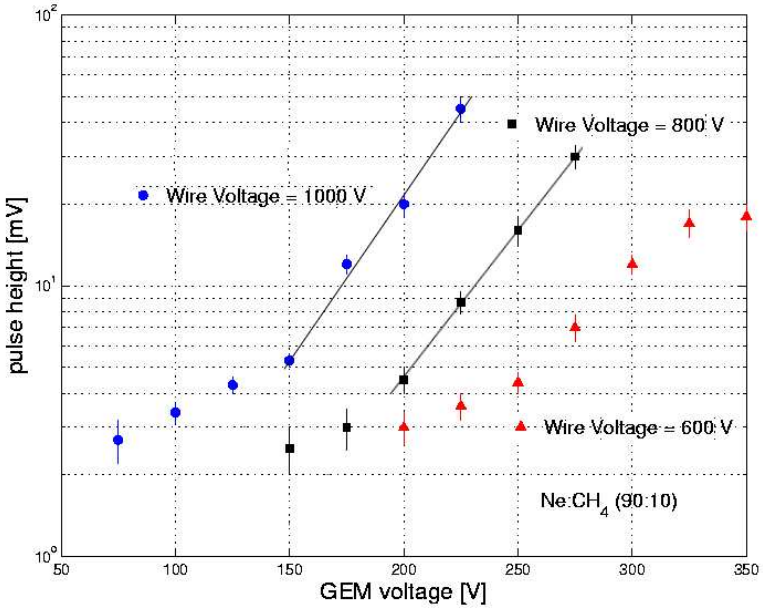

Figure 3-15: Pulse height versus GEM voltage at constant wire voltages in Ne:CH_4 (90:10).

$\frac{\Delta G}{G\Delta V}[\frac{1}{V}]$	Ar:C_2H_6 (50:50)	Ar:CH_4 (90:10)	Ne:CH_4 (90:10)
wires	0.0023 ± 0.0002	0.0045 ± 0.0003	0.006 ± 0.001
GEM	0.008 ± 0.005	0.016 ± 0.004	0.025 ± 0.005

Table 3.2: Values of $\frac{\Delta G}{G\Delta V}$ for the wires and the GEM in each gas mixture.

3.4.3 Comparison of Gases

The two types of gain that enter Eqn. 3.9, G_{wire} and G_0, are related in the same gas through the First Townsend coefficient, $\alpha(E)$:

$$G_{wire} = e^{\int_{rmin}^{rmax} \alpha(E_{wire})dx} \tag{3.10}$$

$$G_{GEM} = e^{\int_{d_{drift}}^{d_{mesh}} \alpha(E_{GEM})dx} \tag{3.11}$$

Eqn. 3.10 can be evaluated using the Diethorn Approximation as discussed in Section 3.4.1. Using the Diethorn Approximation, it is possible to extract the First Townsend coefficient, $\alpha(E)$, which could then be used to evaluate Eqn. 3.11. By averaging G_{GEM} over all successful paths, one can calculate G_0. By including the transfer functions, one obtains G_{eff}, as discussed in Appendix D. Experimentally, we extracted $(\frac{\Delta G}{G\Delta V})_{wire}$ for each gas from Figs. 3-10, 3-12, and 3-14 and $(\frac{\Delta G}{G\Delta V})_{GEM}$ for each gas from Figs. 3-11, 3-13, and 3-15. The values are given in Table 3.2 and shown in Fig. 3-16. We can conclude that the wire and GEM gain are correlated as expected and that Ar:C_2H_6 (50:50) has the lowest gain, followed by Ar:CH_4 (90:10), and that Ne:CH_4 (90:10) has the largest gain of the three gases. Obviously, neon has better amplification features than argon and is well suited for use in new future detectors.

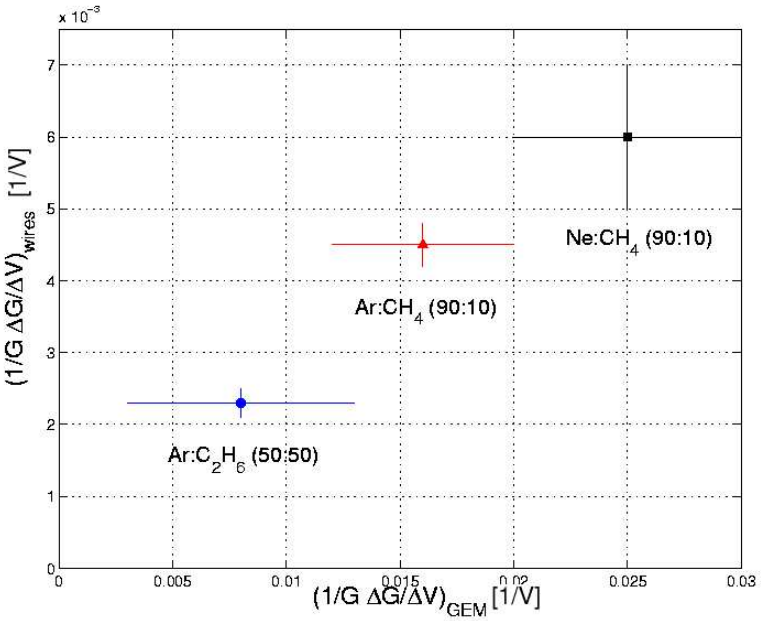

Figure 3-16: Plot of $\frac{\Delta G}{G\Delta V}$ for the GEM versus $\frac{\Delta G}{G\Delta V}$ for the wires in each gas mixture.

3.5 Cosmic Muons

3.5.1 Triggering

Most cosmic muons are minimum ionizing and create tracks which, unlike alpha particles, traverse the entire TPC. Unlike the trigger for the alpha particles, the cosmic rays were triggered by the coincidence of two 2 cm x 2 cm scintillators placed above and below the TPC, as shown in Fig. 3-17. The expected rate of coincidences can be calculated by estimating the solid angle subtended by the scintillators:

$$R = 2I_v \frac{A_1 A_2}{2\pi d^2}, \tag{3.12}$$

where I_v is the vertical muon flux of $\frac{1.08}{minutecm^2}$, A_1 and A_2 are the areas of the scintillators and d is the distance between the scintillators [2]. For my configuration, where $A_1 = A_2 = 4cm^2$ and $d = 35cm$, the expected rate of coincidences is 1 in four hours. At this low rate the percentage of accidental coincidences can be sizeable.

They were measured by observing the coincidences when the scintillators were 1.5 m apart horizontally. No accidental coincidence were seen in 36 hours. The expected

rate of accidentals can be calculated as

$$N_0 = N_1 N_2 (\tau_1 + \tau_2) \tag{3.13}$$

where N_1 and N_2 are the rates of the individual counters and τ_1 and τ_2 are the widths of the discriminated scintillator signals [7]. For these scintillators, N_1 and N_2 were 10 counts/min and 275 counts/min and τ_1 and τ_2 were 23 ns and 64 ns, making the expected rate of accidentals 0.00035 counts/min = 1/48 hours. Therefore, the accidental measurement is consistent with the expected rate.

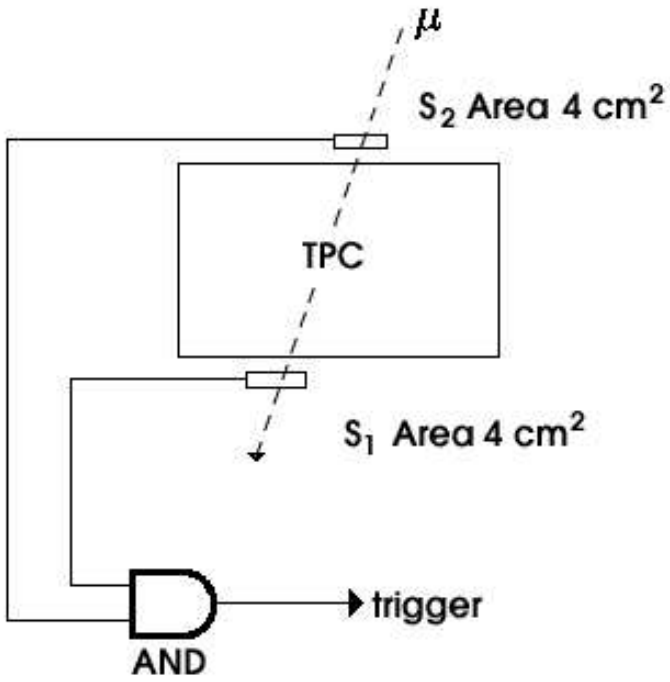

Figure 3-17: Side view of the configuration used for cosmic trigger. The chamber is tilted 90° so that the muons enter the drift region and the electrons drift towards the readout.

3.5.2 Tracks

Since the muon tracks cover the entire length of the TPC, it is not possible to show oscilloscope data for all the wires. Therefore three wires were chosen along the length of the TPC and the signals there were recorded as shown in Fig. 3-19. An example of the pad data for a cosmic ray can be seen in Fig. 3-18.

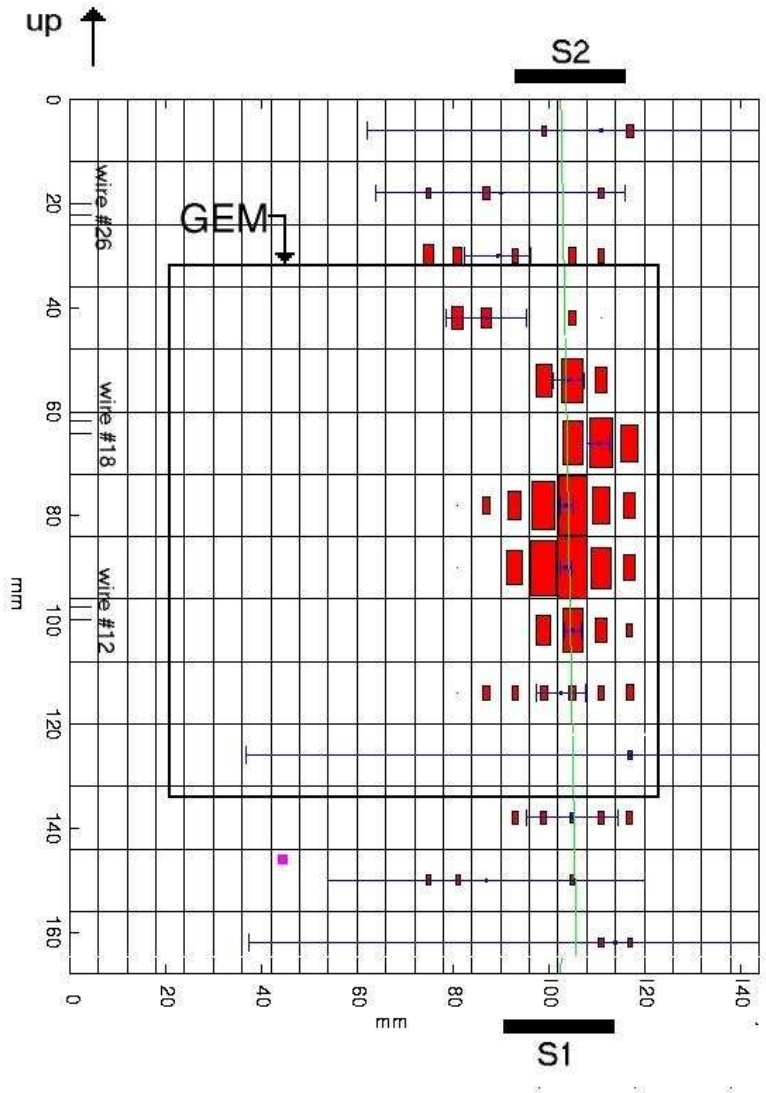

Figure 3-18: Pad data from a cosmic ray muon in Ar:CH_4 (90:10). The fully shaded pad corresponds to a charge of 21.5 pC and charge scales with the shaded area for the other pads.

In order to record the pad data from cosmic events, it is necessary to make some

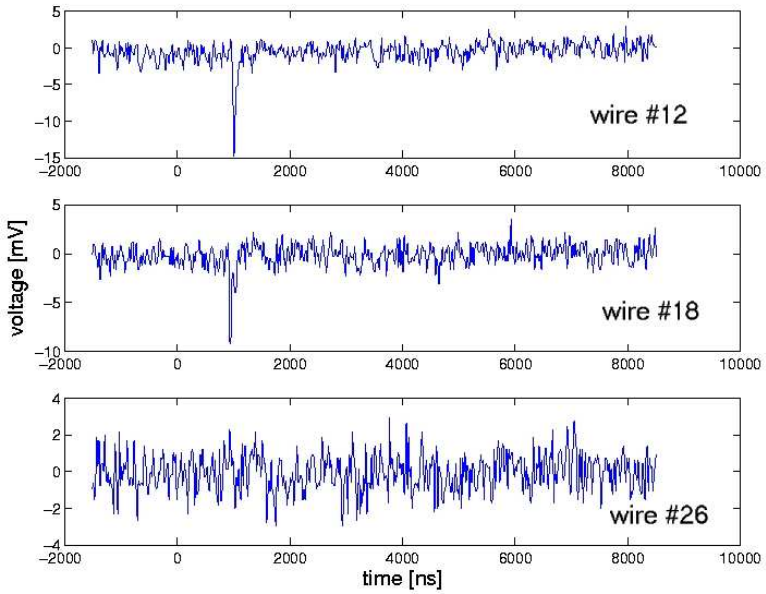

Figure 3-19: Scope data from a cosmic ray muon in Ar:CH_4 (90:10). There is no signal on wire 26 because it is obscured by the GEM.

changes to the electronics. These changes, along with procedures for taking pad data, are given in Appendix E.

This is the beginning of a more detailed study, but together with the alpha tracks, it shows that a GEM amplified TPC can be used as a tracking device.

Chapter 4

Summary

A test TPC was used to study alpha particles and cosmic ray muon tracks detected by GEM amplification. The ranges for the ^{241}Am alpha tracks were determined for gas mixtures of Ar:C_2H_6 (50:50), Ar:CH_4 (90:10), and Ne:CH_4 (90:10), showing the tracking capability of this GEM TPC. The range in these three gases were 2.8 $\pm$ 0.5 cm, 3.2 $\pm$ 0.5 cm, and 4.8 $\pm$ 0.5 cm respectively. These ranges were somewhat smaller than the ranges expected for a 5.5 MeV alpha particle, but consistent between the gases. According the published data, the ranges measured here correspond to an energy of 4.3 MeV [1], so we can conclude that 1.2 MeV is lost in the thickness and coating of the source. Alpha particles were also used to study the gain of the GEM as well as the wires. Both the GEM gain and the wire gain was smallest for Ar:C_2H_6 (50:50), larger for Ar:CH_4 (90:10), and largest for Ne:CH_4 (90:10), suggesting that a neon mixture is well suited for use in future detectors. The TPC was used to detect minimum ionizing particles by recording cosmic ray tracks in Ar:CH_4 (90:10), which is closer to the aim of using it in a collider.

There is much more that could be done with this TPC. In the future, further work could be done with cosmic ray muons and it would be interesting to study tracks made by an ultraviolet laser. Also, the TPC could be studied with multiple GEMs, both with and without the wires and the timing information could be improved by using TDCs.

Appendix A

Stretching the GEMs

The GEMs in the TPC are spaced on the order of 1mm; therefore, it is necessary that the GEMs are stretched so they are very flat. The stretching is performed using thermal expansion while attaching the foils to G10 frames using epoxy.

In preparation, a piece of lucite 155mm x 155mm and 3mm thick is placed in a freezer ($\sim$-10°C). It is placed in a plastic bag so that condensation does not form on the plate. A hot plate is warmed to $\sim$60°C. Double sticky tape is attached to the kapton foil around the outside of the GEM. The tape is stuck to the cold lucite plate and allowed to come to room temperature. This prestretches the GEM.

Next, the edge of the GEM foil and frame are roughened with sandpaper and cleaned with isopropyl alcohol so that the epoxy will adhere. A thin layer of epoxy is spread around the edge of the GEM, being careful not to get any epoxy on the GEM itself. The G10 frame is placed carefully on the epoxy. It is all placed on the hot plate, and lead bricks are used to ensure contact between the GEM foil and the frame. The heat from the hot plate further stretches the GEM and helps the epoxy cure.

After 24 hours, the epoxy has cured and the GEM is stretched. It is now necessary to remove the lucite plate. Isopropyl alcohol can be useful for loosening the adhesive tape. The best results were obtained by prying the lucite off with a thin blade such as a razor blade or pocket knife. The thickness of the lucite is very important in this step. Previous attempts with thicker lucite sheets resulted in damage to the

foil. I strongly recommend that you practice this procedure with a kapton foil before attempting to stretch a GEM.

A schematic of the procedure is shown in Fig. A-1:

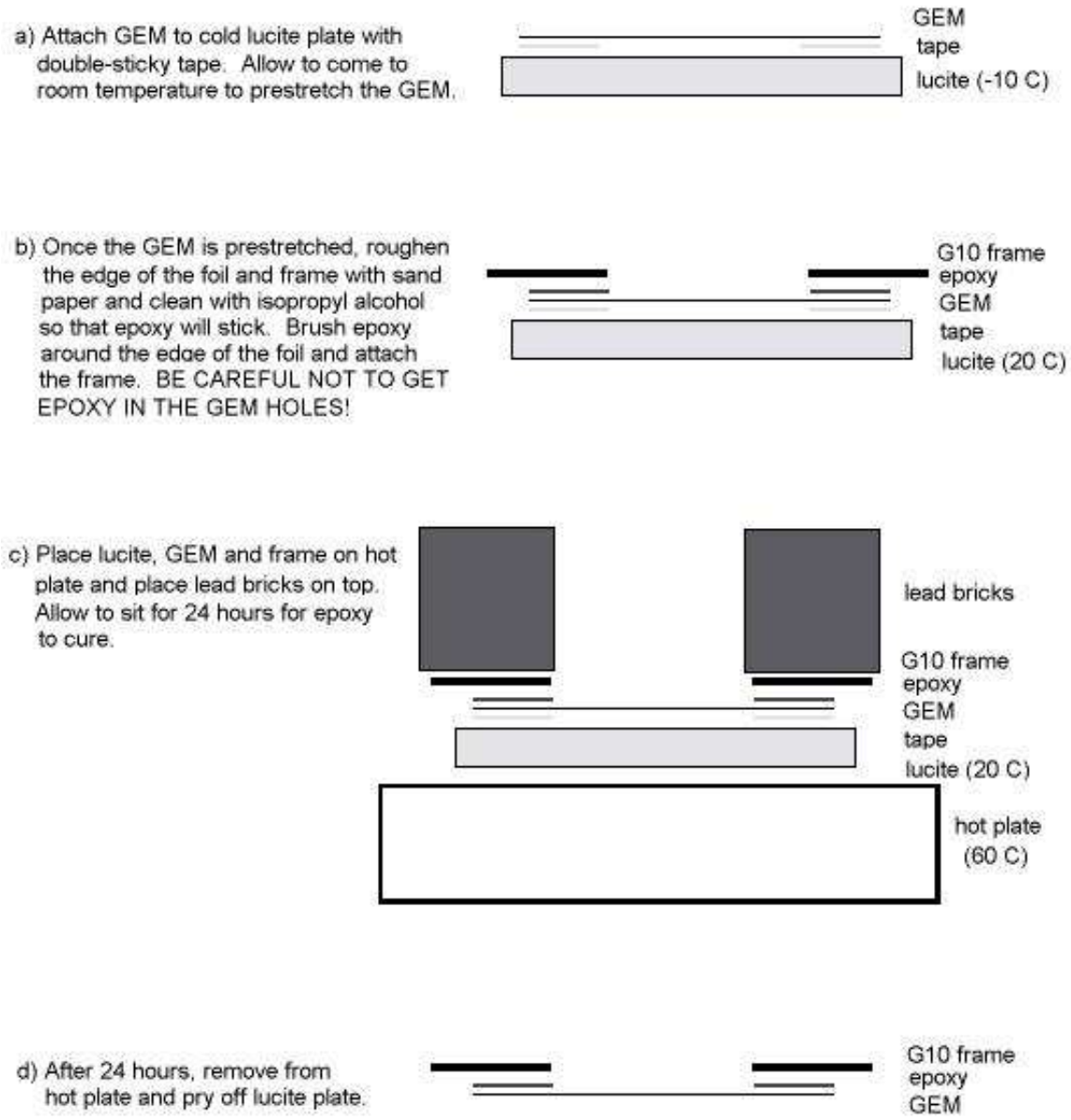

Figure A-1: Schematic of procedure used to stretch GEMs.

Appendix B

Electrical Testing of GEMs

After the GEMs are stretched and attached to the frames, it is necessary to test them electrically. In dry air, a GEM must be able to hold 400V with less than 7nA of current. At 500V, the current must be less than 10nA. The GEMs were tested in dry nitrogen using the setup shown in Fig. B-1. The results of the testing for seven GEMs is shown in Table. B.1. GEM 5 was used for measurements in this thesis.

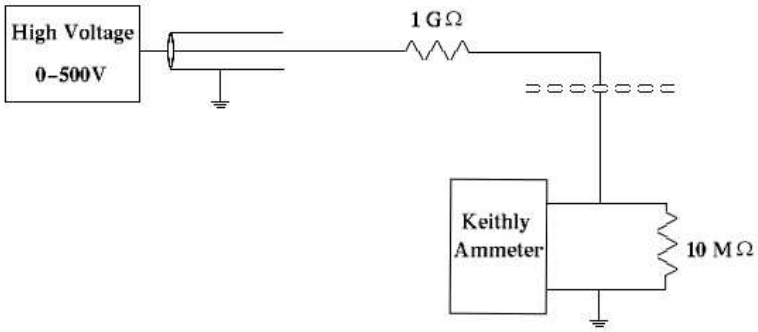

Figure B-1: Electric setup used to test GEMs.

	GEM 1	**GEM 2**	GEM 3	GEM 4	GEM 5	**GEM 6**	**GEM 7 (poorly glued)**
100V	< 0.001	< 0.005	< 0.005	< 0.02	< 0.02	< 0.02	< 0.02
200V	< 0.001	< 0.005	< 0.01	< 0.02	< 0.02	< 0.02	< 0.02
300V	< 0.001	< 0.005	< 0.01	< 0.02	< 0.02	< 0.02	< 0.02
400V	< 0.001	< 0.005	< 0.02	< 0.02	< 0.02	< 0.02	**6.0 ± 0.1**
500V	< 0.001	> 45	< 0.01	< 0.02	< 0.02	< 0.02 **(sparked)**	**7.9 ± 0.1**

Table B.1: Results of electrical testing of GEMs. All currents in nA.

Appendix C

Measuring Hole Diameter

The diameter of the GEM holes was measured by comparing a grating of known pitch to the holes using a digital camera and microscope. A grating with a pitch of 1000 lines per inch was placed under the microscope and a picture was taken with a digital camera. Without changing any settings, the grating was replaced with the GEM, and pictures of the GEM holes were taken with the same camera. The lighting was arranged so that the GEMs could be lit from above, below or both. When lit from above, it was possible to see the large holes in the copper, but not the smaller holes in the kapton. When lit from below, the smaller holes in the kapton were visible, but not the large holes in the copper. When the GEM was lit from both above and below, it was possible to see both holes.

Since the size of the grating is known, it is possible to determine how many microns corresponded to one pixel. Then by counting the pixels in the GEM hole, one knows the diameter of the hole.

Pictures were taken both with a microscope in our lab and with a microscope in the Microsystems Technology Laboratory. A picture taken with our microscope is shown in Fig. C-1; the black crosses in the picture represent the measurements of the diameter. A picture taken with the Microsystem Technology Laboratory's microscope is shown in Fig. C-2. The diameter of the large hole in the copper was determined to be $72 \pm 1\mu m$; the diameter of the small hole in the kapton was determined to be $41 \pm 1\mu m$.

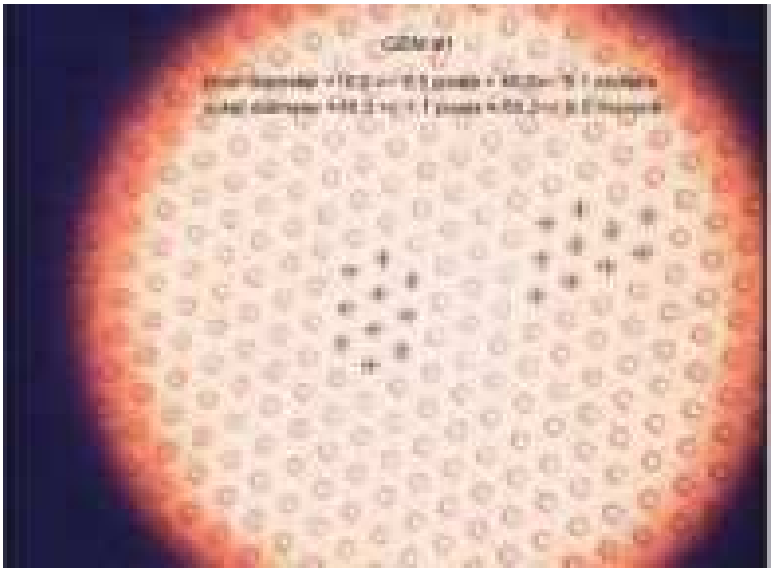

Figure C-1: Digital photograph of GEM taken at our laboratory.

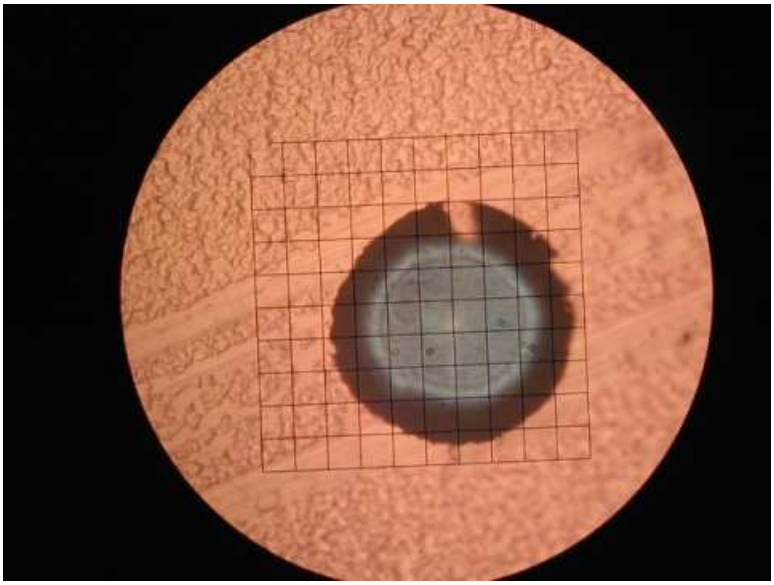

Figure C-2: Digital photograph of a GEM taken at the Microsystems Technology Laboratory.

Appendix D

Results from Maxwell 3D

Peter Fisher used the program Maxwell 3D to simulate the expected gain from the GEMs [4]. For the geometry described in this thesis, the simulated gain is given in Table D.1. It is important to note that Maxwell 3D does not include the surface charges in these simulations.

Maxwell 3D bases these simulations on calculations of the equipotential lines and the electron trajectories in the GEM holes. These quantities can be seen in in Figs. D-1 and D-2.

The gain is calculated by integrating Eqn. 3.5 assuming that the First Townsend coefficient, α is given by Fig. D-3 [5].

V_{GEM} [V]	G_{sim} in Ar	G_{sim} in Ne
275	4.1	5.8
300	5.4	7.2
350	8.0	7.4
450	45	17.2
550	97	19.2

Table D.1: Simulated gain for a GEM in argon and neon.

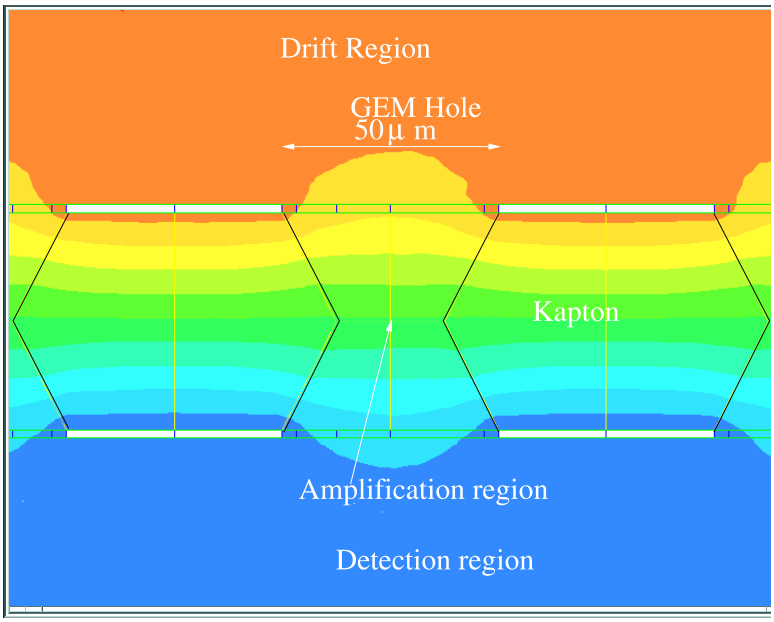

Figure D-1: The equipotentials near a GEM hole as calculated by Peter Fisher using Maxwell 3D [4].

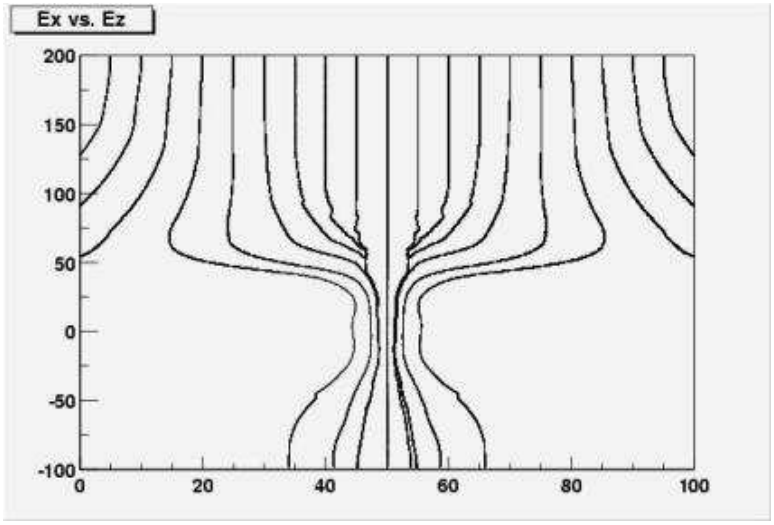

Figure D-2: The electron trajectories near a GEM hole as calculated by Peter Fisher using Maxwell 3D [4].

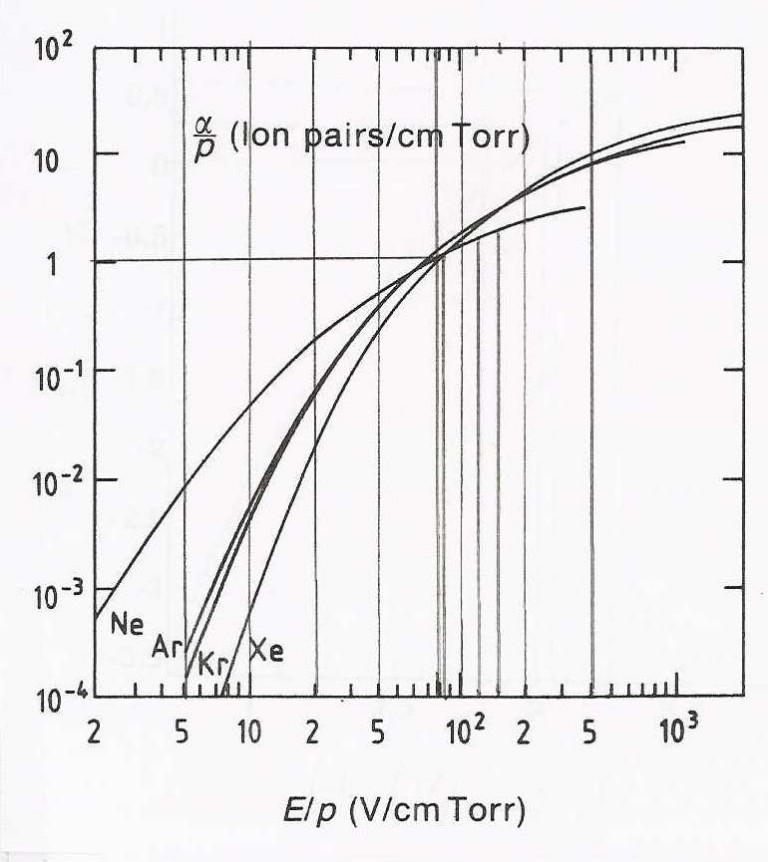

Figure D-3: The First Townsend coefficient in different noble gases [5].

Appendix E

Procedure for Taking Pad Data

E.1 Pad data for Alphas

These instructions for the collection of alpha tracks are taken from Josh Thompson's senior thesis [2].

An overall note: The programs will at various times before data collection ask for confirmation to replace various files. The user should click "Replace" to confirm the replacement of these files.

Setup

1. Power on NIM and CAMAC crates
2. Power on scope (Trigger should be External)
3. Do not power on ± 5 V or HV
4. Make sure the needle valve on the TPC is open.
5. Start gas flowing
6. On NIM crate, one Lemo cable is plugged into the ECL-NIM-ECL module. The position of this cable determines the trigger wire.
7. Set switch on 322G Logic unit (NIM) to "OR" position.

8. If not already loaded, load the `alpha_readout_continuous_tdc.vi` program in LabView.

Procedure

9. Make sure the button "Take Scope Data" is illuminated.

10. If you wish to collect data points one at a time, place the switch in the middle of the screen in the "User Iterate" position. If you wish to have data continuously collected, place the switch in the "Continuous" position.

11. A new calibration is needed each time the program is run, so make sure the switch labelled "Take New Calibration?" is on. To take the calibration, the cable from the pulser to the logic gate must be switched from $\overline{3}$ to 1.

12. Run the program by clicking the white arrow in the upper left hand corner.

13. A box pops up asking for a file name. This will be the name of the pad data file. The name must end in ".log".

14. A calibration is performed which takes about 5 minutes. This stage is over when the program asks you to confirm replacement of "trv_all.log".

15. Pedestals are measured, ending with the program asking to replace "pedestal.log".

16. Now that the calibration is complete, move the cable from the pulser to the logic gate back to $\overline{3}$ and move the switch on the 322G to "AND."

17. Turn on the HV and ± 5 V.

18. If you are in "User Iterate" mode, data is collected by clicking the "Iterate" button at the center of the screen. If you are in "Continuous" mode, data is already being taken.

19. To stop taking data, click "Cancel."

20. Remember to copy "trv_all.log" to "dtmmddyy_cal.log" before running the program again.

E.2 Pad data for Cosmics

These instructions for the collection of cosmic tracks are taken from Josh Thompson's senior thesis [2].

1. Turn on power to the CAMAC and NIM crates. Turn on power to the oscilloscope.
2. Make sure the needle valve on the TPC is open.
3. Start gas flow.
4. If not already loaded, load the `cosmics_readout_tdc.vi` program in LabView.
   (a) If the CAMAC power has been cycled since the last calibration, turn on the switch labelled "Take New Calibration?" If no new calibration is needed, then turn this switch off.
   (b) Make sure the CAMAC slots are set correctly (they should be).
   (c) Adjust the Gate and Delay settings if necessary. The default of a 4000 ns gate after a delay of 200 ns is probably correct.
   (d) Run the program by clicking the white arrow in the upper left hand corner.
5. You will be prompted for the datafile name. Enter a name in the dialog box.
6. As instructed by the computer program, disconnect the two analog inputs to the 2249 ADC. Replace them with 50Ω terminators.
7. Set the switch on the 322G logic unit to the OR position.
8. Hit the "Done" button on the computer. The computer then takes a number of data points for 2229 ADC pedestal subtraction.

9. The computer will show another box indicating that you should reconnect the ADC analog inputs.

10. After reconnecting the inputs, put the logic unit in OFF mode.

11. Hit the "Done" button on the computer. You will be prompted to replace pedestal.log. The computer then does a calibration which takes about 5 minutes.

12. You will have to confirm the replacement of a file. The computer then takes data for FERA pedestal subtraction. You will know this is complete when a box comes up asking for confirmation to replace "trv_all.log."

13. At this point, the computer is trying to collect data. Turn on the high voltages. Also turn on the low voltage power supply.

14. Flip the logic unit to the AND position to trigger on coincidence of the scintillators.

E.3 Converting from Wire-based Trigger to Scintillator-based Trigger

To convert from the wire-based alpha trigger to the scintillator based cosmic trigger it is necessary to make some changes to the CAMAC and NIM electronics. It may be useful to refer to the diagrams the electronics as shown in Figs. E-1 and E-2 [2].

1. For measurements with alpha particles the readout cables from the pads to the FERAs start on the 14th pin from the chamber. To take measurements with cosmics the cables should start at the 4th pin from the chamber.

2. For alpha particles the first three adjacent wires in front of the alpha source are read out on the scope. However, since the cosmic tracks are longer, it is important to stagger the wire signals along the length the track.

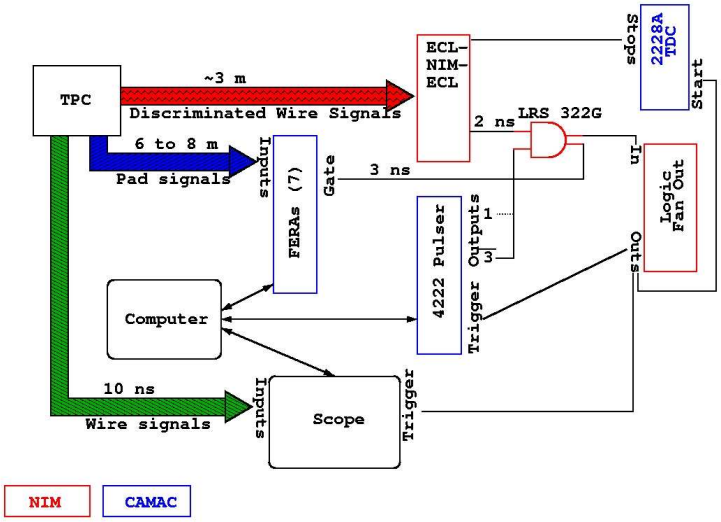

Figure E-1: Diagram of readout electronics for alpha measurements [2].

3. On the side of the PDG 4442 there are some switches that need to be changed. To access the switches, it is necessary to remove the module from the CAMAC crate. For measurements with alphas, the gate settings should be on Normal mode for all four channels and for measurements with cosmics the gate settings should be Gate mode on all four channels. The other switches do not change.

4. Plug the Lemo cables from the scintillators into the top two sections of the 428F Fan Out.

5. Connect one of the outputs from the coincidence gate into the trigger for the 4222 Pulser.

6. Connect the output labeled 1 on the 4222 Pulser to the gate for the FERAs.

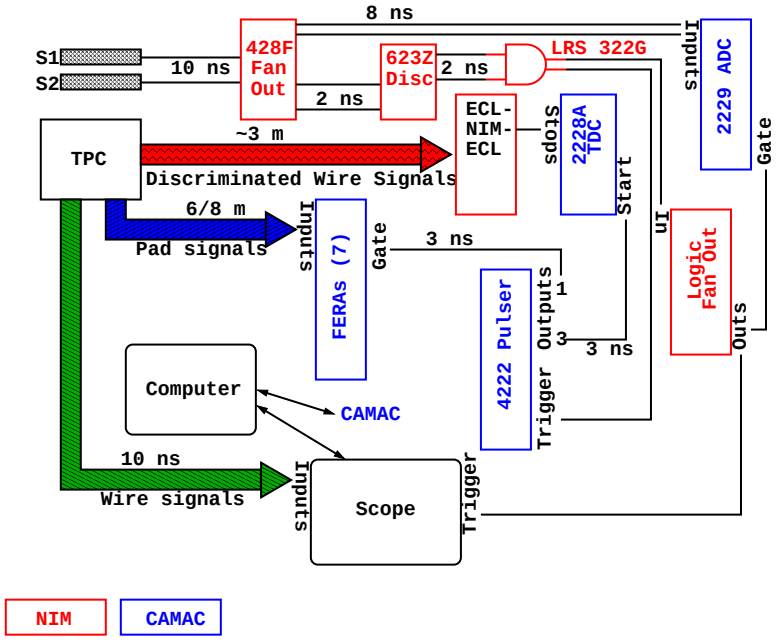

Figure E-2: Diagram of readout electronics for cosmic ray muon measurements [2].

Bibliography

[1] M. J. Berger, et al. Stopping power and range tables for electrons, protons and helium ions. *http://physics.nist.gov/PhysRefData/Star/Text/contents.html*, 2002.

[2] Joshua Michael Thompson. A Readout System for a TPC Detector. Senior Thesis, Massachusetts Institute of Technology, Physics Department, June 2002.

[3] Ulrich Becker. MIT LNS Drift Gases R&D Experiment. *http://cyclo.mit.edu/drift*, 2002.

[4] Peter Fisher. Simulations of electric field in a GEM using Maxwell 3D Field Simulator by Ansoft Corporation. *MIT*, 2002.

[5] W. Blum and L. Rolandi. *Particle Detection with Drift Chambers.* Springer-Verlag, Berlin, 1994.

[6] U. Becker and V. Koutsenko. "An Antimatter Spectrometer in Space", V. M. Balebanov, et. al., proposal. 1994.

[7] William R. Leo. *Techniques for Nuclear and Particle Physics Experiments.* Springer-Verlag, Berlin, 1994.

[8] DuPont. *http://www.dupont.com/kapton/*, 2002.

[9] S. Bachmann, A. Bressan, S. Kappler, B. Ketzer, M. Deutel, L. Ropelewski, F. Sauli, E. Schulte. Development and applications of gas electron multipliers. *Nuclear Instruments & Methods in Physics Research*, 2001.

[10] N. Ghodbane. The TESLA Time Projection Chamber. 2002.

[11] R. J. Madaras et al. Spatial resolution of the PEP-4 time projection chamber. *IEEE Trans. Nucl. Sci.*, 30:76–81, 1983.

[12] P. S. Marrocchesi et al. The spatial resolution of the ALEPH TPC. *Nucl. Instrum. Meth.*, A283:573–577, 1989.

[13] Y. Sacquin. The DELPHI time projection chamber. *Nucl. Instrum. Meth.*, A323:209–212, 1992.

[14] http://alephwww.cern.ch/ALEPHGENERAL/reports/alephnum/alephnum.html. *CERN.*

[15] http://delonline.cern.ch/delphi$specific/cp/monitor/presenter/help_files/tpc_descrip.html. *CERN.*

[16] H. Wieman et al. STAR TPC at RHIC. *IEEE Trans. Nucl. Sci.*, 44:671–678, 1997.

[17] Mr. deOliviera and F. Sauli. Standard GEMs designed by F. Sauli and manufactured by Mr. deOliviera. *CERN.*

[18] M. Ziegler, P. Sievers and U. Straumann. A triple GEM detector with two-dimensional readout. *Nuclear Instruments & Methods in Physics Research*, 2001.

[19] S. Bachmann, A. Bressan, M. Capeans, M. Deutel, S. Kappler, B. Ketzer, A. Polouektov, L. Ropelewski, F. Sauli, E. Schulte, L. Shekhtman and A. Sokolov. Discharge studies and prevention in the gas electron multiplier (GEM). *Nuclear Instruments & Methods in Physics Research*, 2002.

[20] T. Behnke, S. Bertolucci, R. D. Heuer and R. Settles. TESLA, Technical Design Report. *http://tesla.desy.de/new_pages/TDR_CD/start.html*, 2001.

[21] U. Becker, et. al. To be published.

[22] Teresa Fazio. Pressure changes and saturation of gas gain in conventional wire detectors. Senior Thesis, Massachusetts Institute of Technology, Physics Department, January 2002.

[23] W. Diethorn. A methane proportional counter system for natural radiocarbon measurements. *USAEC Report NY06628*, 1956.